The Impact of Trade on Development: Evidence from Pastoralist Practices on the Ancient Silk Road

Michelle S. Lam*, Bunyada (Mos) Laoprapassorn†

October 24, 2022

Abstract

This paper studies the long-term effect of trade on development. We approach this question in the context of the ancient Silk Road, examining whether the locations along the highland Silk Road continue to be relatively more developed than other locations in the highland region along the Inner Asia Mountain Corridor that were not on the ancient Silk Road. We proxy for modern development using high-resolution satellite imagery. To provide a causal effect between proximity to the Silk Road and modern development, we adopt a novel instrumental variable, using a simulated seasonal mobility pattern of the nomadic pastoralists from Frachetti et al. (2017) as an instrument for the location of the Silk Road sites. We find a significant and robust positive relationship between proximity to Silk Road sites and modern development measures; an increase in the distance to the Silk Road by one standard deviation decreases the night lights intensity by 10.0%. Based on the elasticity of night lights with respect to GDP in the literature, this corresponds to a decrease in GDP of about 4.1%-9.7%.

*msll@umich.edu

†bunyada@umich.edu

‡We are grateful to Sebastian Sotelo, Andrei Levchenko, Dominick Bartelme, Hoyt Bleakley, Jagadeesh Sivadasan, Lauren Falcao Bergquist, Jon-Denton Schneider, H2D2 seminar participants, Philadelphia Federal Reserve seminar participants, Morgan Kelly, Dean Yang, Robert Venigye, and Michael Frachetti for all of their helpful comments and suggestions.

1 Introduction

What is the long-term impact of historical trade on modern development? We approach this question in the context of the overland ancient Silk Road, the ancient trade route across Eurasia. Although the development of long-distance maritime technology in the sixteenth century has rendered the overland Silk Road trade route obsolete, path dependence could result in a persistent effect on economic activity along the ancient Silk Road trade route. Therefore, we seek to examine whether, five centuries after the decline of the overland ancient Silk Road trade, places in close proximity to the ancient Silk Road continue to be more developed relative to places that were not on the Silk Road. In particular, we focus on the long-term impact of the ancient Silk Road in the Inner Asia Mountain Corridor (IAMC), which spans modern-day Afghanistan, China, India, Kyrgyzstan, Kazakhstan, Pakistan, Tajikistan, and Uzbekistan.[1]

Studying the impact of the ancient Silk Road trade on modern development along the IAMC is challenging because of the limited data availability. We overcome the data constraints by utilizing high-resolution satellite imagery. Our main analysis uses the intensity of night lights to proxy for the level of modern development. Remote sensing of nighttime light emissions from the Earth's surface has been widely used as a proxy for economic activity and economic development where conventional measures such as GDP are not available. In addition to its availability on a high spatial resolution, the night lights data allow researchers to circumvent concerns about the manipulation, censoring, and measurement errors in official statistics, which may be non-trivial issues in the context of the geographical area we study. Nevertheless, acknowledging the limitations of night lights data, we also use population density and data on urbanized lands as alternative measures of modern development in our supplement analysis.

To provide evidence of the causal relationship between proximity to the Silk Road and modern development level, we adopt a novel instrument for the locations of the Silk Road. We take advantage of the characteristics of the IAMC and its inhabitants to construct an instrument that provides exogenous variation in the locations of the Silk Road sites. Due to the harsh geographical conditions and the strong pastoralist tradition along the IAMC, highland Silk Road networks emerged in relation to seasonal mobility patterns of the nomadic herders (**?**). We use the simulated mobility patterns of the nomadic herders, which are generated based solely on the seasonal pasture quality, to provide variations in the placement of the Silk Road sites that do not arise from ease of travel. Conditional on the location's suitability for growing crops, our instrument only affects modern development level through the ancient Silk Road trade.

We conduct the main analysis in this paper using a grid of 0.167 degrees by 0.167 degrees grid cells covering the highland region of the Silk Road. We find a negative and significant relationship

[1] We choose to study the IAMC as it contains unique conditions for the existence of nomadic pastoralism, which are keys to our identification strategy. We explain further details about the instrument in Section 4. Nomadism refers to not having a fixed place of abode, and pastoralism refers to people making their livelihood by herding animals.

between distance to the Silk Road and modern development level; as distance to the Silk Road increases by one standard deviation, the night lights intensity decreases by 10.0%. Based on the elasticity of night lights with respect to GDP in the literature, a 10.0% decrease in night lights intensity corresponds to a decrease in GDP of about 4.1%-9.7%.[2] Our results are robust across different measures of modern development, with a one standard deviation increase in distance to the Silk Road resulting in a 85.5% decrease in population density, and a 12.3% decrease in the percentage of land covered by cultivated land or artificial surfaces.

This paper makes three main contributions to the economics literature. The first contribution of this paper is adding to the sparse literature on how trade routes may have a persistent effect on development, even when the trade routes are no longer relevant to trade patterns in the period of development that is of interest. To do this, this paper also draws on the literature studying path dependence and the impact of durable built infrastructure, such as **?**, **?**, **?**, **?**, and **?**.

Second, this paper is one of the first studies on the ancient Silk Road using modern econometric techniques and detailed satellite data. Our paper adds to the small but growing economics literature that studies ancient civilizations using limited archaeological records: **?** study Ancient Roman roads, **?** also study Ancient Roman roads, **?** study British and French urbanization from 117 to 2012, **?** study the Ancient Phoenicians around ninth century BCE, and **?** study Assyrian merchants in nineteenth century BCE. Of particular interest is **?**, who also study the persistence along the ancient Silk Road. To study the long-term consequences of the ancient Silk Road on economic activities, they regress the night lights intensity outcome variable per grid on the presence of the Silk Road in four bins: 0-50km away, 50-100km away, 100-150km away, and 150-200km away, and find there is a persistent and positive association in areas that are within 50km to the ancient Silk Road. While they have conducted exercises to provide suggestive evidence about the long-term impact of the ancient Silk Road on modern economic activities, the nature of the specification in their paper does not allow them to establish a causal relationship. Our study differs from theirs in two main respects: 1) our perspective that the Silk Road is a dynamic network of paths, leading us to avoid using static routes generated from least-cost paths calculation like those in **?**; because of this, 2) we introduce a unique simulated instrument for distance to Silk Road sites to establish a causal link.

This paper is part of a strand of research that uses detailed satellite data, including papers such as **?**, **?**, and **?** that use night light data to study development intensity. More recent papers have begun to use daytime imagery, often alongside machine learning, to extract features such as farmed land, building density, vegetation type, transportation, and roof types to study the economic development of areas that may otherwise have sparse data or data that is not easily comparable across borders. Such papers include **?** **?**, and **?**.

[2]Literature has found the elasticity of night lights with respect to GDP to be around 0.41-0.97 (**??**).

The third contribution of this paper is introducing novel-to-economics mapping simulation techniques to generate a valid instrument for the impact of ancient trade routes on modern development. Lack of direct and accurate information is a major challenge when studying events from antiquity, but depending on the right conditions, a study may be able to use modern simulation techniques to generate patterns of movement that we can plausibly argue to be similar to those experienced in antiquity. In this paper, we take advantage of the importance of the highlands area to the overland Silk Road trade and the highlands' continuing primary usage by herders and their flocks. Because of this, we are able to use modern satellite imagery to produce herding movement simulations comparable to those experienced in the ancient Silk Road heyday, and then use these calculated flows to instrument for the locations of the Silk Road sites.

Section 2 of the paper introduces the relevance to the background of the ancient Silk Road. Section 3 describes the data and how we construct data for each unit of observation. Section 4 details the empirical strategy, describing the instrument that we use and the various robustness checks we perform. Section 5 discusses possible mechanisms through which the ancient Silk Road impacts modern development. Section 6 concludes.

2 Background

Despite its name, the "ancient Silk Road" does not refer to a physical road, nor is there an unambiguous route that researchers agree to be definitively used during the centuries of overland Silk Road trade. Maps of the ancient Silk Road, such as Figure 1 pick important nodes at the researcher's discretion and often deploy least-cost methods based on terrain and elevation to determine where a likely path would lie. More accurately, one may think of the Silk Road as "skein of routes linking many entrepots" connecting East Asia to the Mediterranean and a phrase that represents the dynamic cultural phenomenon that connected Eurasia's people, ideas, and goods together **??**. Thus, when this paper mentions the ancient Silk Road, we are not referring to a physical road in particular, but to the dynamic network of paths identified through known historical sites.

2.1 Definitions

The term Silk Road (in German, "Seidenstrasse") was coined in 1877 by a German geographer, Ferdinand Freiherr von Richthofen. At the time, this term narrowly referred to routes under the Han Empire (206 BCE to 220 CE) which commonly traded Chinese silk (**?**). However, since this initial usage, the Silk Road has evolved to describe diverse goods and ideas exchanges ranging over diverse geographies and long stretches of time–thousands of years and tens of thousands of kilometers. Travelers on the ancient Silk Road carried precious goods such as textiles, metals, stone, ceramics, perfumes, and horses, disseminated religious beliefs like Buddhism, Islam, Christianity, and technological advancements like paper, gunpowder, calendrical sciences, and medicine. As such, although the ancient Silk Road is often represented as a set of unchanging least-cost paths

Figure 1: Silk Road Routes

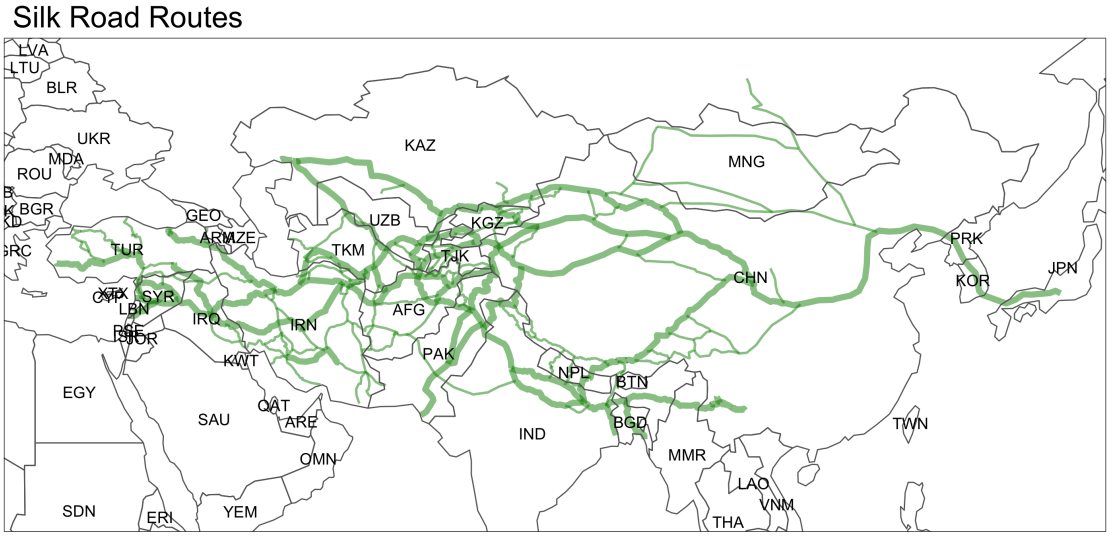

Notes: This figure presents hypothetical Silk Road routes compiled in **?**. The thicker lines denote the main corridors; the thinner lines denote the sub-corridors. Williams first chose important nodes such as prominent cities and mountain passes, and then chose pathways considering smaller-scale sites and the ease of travel between segments. The scope of the routes spans from central China to the eastern Mediterranean, but does not address Mongolia and the routes between East Asia (China, Japan, Korea). The routes are also sparse in South Asia.

through important nodes as in Figure 1, the ancient Silk Road is more accurately thought of as a dynamic network that connected various geopolitical concerns at different settings in time (**?**). Therefore, in this paper, unless otherwise stated, the terms "road", "path" and "route" do not refer to an explicit, physical set of roads. Rather, we acknowledge the Silk Road dynamically evolved and shifted with the populations that inhabited the region, a trait that we use in this paper to arrive at an instrument.

This study exploits the mobility patterns of pastoral nomads to form an instrument. Following **?** *The Archaeology of Mobility: Definitions and Research Approaches*, "pastoral nomadism" is the "general term for mobility centered on maintenance and welfare of flocks or herds." The word "pastoral" describes the herding, and the word "nomadism" describes the high mobility and impermanence of settlements. It is useful to make the distinction between pastoral nomads and hunter-gatherers, who are often thought to be similar but are distinct (**?**). First, hunter-gatherers move towards resources for humans, whereas pastoral nomads move towards resources for flocks, independent of human resources. Second, hunter-gatherers have typically varied mobility to secure different resources, whereas pastoral nomads are only interested in grazing resources. As such, the former's migration patterns are more complex compared to the latter's, which tend to be more predictable and can be simulated with greater confidence.

Seasonal migration, also referred to as transhumance, has two differentiating terms (**?**). Vertical transhumance describes seasonal movements in mountainous areas where the snow in the winter forces the flock to move to the lowlands meadows, but in the warmer weather, the flocks move back to the highland pastures. Horizontal transhumance describes movement at around the same elevation even despite untoward weather. In this paper, following **?**, we define highland to be between 750m and 4,000m in elevation.

The area that we study in this paper is referred to as the Inner Asia Mountain Corridor (IAMC). The wide-ranging IAMC stretches from the Hindu Kush mountain range in present-day Afghanistan and Pakistan to the Altai Mountains in Siberia. The IAMC also spans the modern-day countries of China, India, Kyrgyzstan, Kazakhstan, Tajikistan, and Uzbekistan. Before the development of reliable, long-distance maritime routes in the sixteenth century, any trade between East Asia and the Mediterranean had to pass through the long overland routes in the IAMC. The IAMC's varied geography of deserts, steppes, and tall mountain ranges coupled with fertile valleys, oases, and inland deltas gave rise to both vibrant nomadic pastoralist and sedentary agricultural traditions (**?**). In the IAMC, vertical transhumance is the dominant seasonal migration pattern and, thus, the main focus of this paper. We use the small-scale, dynamic vertical transhumance routes of nomadic pastoralists on the highland steppes to study the impact of the ancient Silk Road on modern development.

In summary, using terms as developed by previous scholars across varied disciplines, we use the pastoral nomads' patterns of vertical transhumance in the Inner Asia Mountain Corridor to establish a causal relationship between the ancient Silk Road and modern development.

2.2 History

Silk Road in Six Periods

Evidence of long-distance trade in Eurasia stretches as far back as the fourth millennium BCE, the period which ushered in the Bronze Age and in which writing was invented. One can divide the ancient Silk Road's history into roughly six periods (**?**). The first period, which spans from c. 3000 BCE to c. 300 BCE, is characterized by the expansion of farmers and herders out onto the steppe geographies in Central Asia by taking advantage of the new wheel and wagon technologies discovered c. 3500 BCE. These populations became the first nomadic pastoralists on the steppe.

The second period, lasting from c. 300 BCE to 300 CE, may be thought of as the "Classical Silk Road" period in which the broad area between the Mediterranean and China fell under the centralized control of a few empires. Zhang Qian, a government minister, was dispatched by the Han dynasty in 139 BCE to serve as an imperial envoy to Central Asia. Qian's trip has often been credited with stimulating the opening of different empires and Central Asia to transcontinental trade.

The third to fifth centuries CE was a "dark age" in some sense with the collapse of the western Roman Empire and the fall of the Han empire. However, the Silk Road trade still flourished, with Persians and other Central Asians taking control of the flows.

The fourth and fifth periods of the Silk Road occurred from the sixth to fifteenth centuries CE. They are characterized by the continued expansion of Persians and Arabs in Central Asia and the reunification of China again by the Sui and Tang dynasties and their cosmopolitan tastes. This is then followed by the domination of the Mongol empire over Eurasia.

The last period began in the sixteenth century CE. This period had two major developments: improvement in long-distance maritime technology such that ships were more efficient than overland caravans, and increased security of traveling via the Black Sea. These two developments led to the decline of the overland Silk Road, leading to a simultaneous decline of nomad-steppe culture in Central Asia (**??**).

Nomadic Pastoralists on the Silk Road

Early scholarship on the ancient Silk Road in Central Asia focused on lowland oases where the agricultural tradition is strongest, because they are still heavily populated today and more easily accessible to study. However, with more archaeological work in more remote locations, historians in the past decades have identified more Silk Road sites in the highland mountains. In doing so, they continue to reaffirm the hypothesis that the nomadic pastoralists contributed significantly to the development of the highland Silk Road geography (**?**). Generally, pastoralists in the IAMC would herd their livestock in the mountainous regions to feast on the productive grassland in the summer months and retreat to the lowland oases to weather the winter months. As the grazing herd moved to the productive grassland through the mountainous regions, mobile pastoralists followed. Evidence suggests that these small-scale mobility patterns and subsequent paths formed influenced the formation of the macro-scale Silk Road network (**?**). Trade was most likely conducted in short stages: sold at one node, transported to the next node by following the paths influenced by the nomadic pastoralists, resold at that node, and so forth (**?**).

3 Data

3.1 Data Sources

Examining the relationship between the ancient Silk Road trade and modern level of development requires data on the locations of the Silk Road and fine-level geospatial data on modern development and other characteristics of the areas. We outline below the primary datasets that we use.

Silk Road Sites: Data on locations of Silk Road sites come from Old World Trade Routes (OWTRAD) Project (**?**), a public-access aggregator of geo-referenced and/or chrono-referenced

data of nodes between Eurasia and Africa ranging from 4,000 BCE to 1820 CE, and from **?**, a study of the Silk Road sites done on behalf of International Council of Monuments and Sites. Compiled by historians and archaeologists, the OWTRAD Gazetteer and the ICOMOS study include locations such as current and past settlements, oases, temples, rest houses, markets, forts, river and mountain crossings. As of writing, these databases combined had over 16,000 entries. We follow **?** and extract 258 sites by choosing only sites that are on the IAMC, collapsing duplicate observations which differ only in name, and removing sites that were entered solely to facilitate the generation of a Silk Road path. We further subset to include only the 254 sites situated between 750m and 4,000m in elevation.

Table 1 summarizes the final count of the Silk Road sites by country and node types. Figure 2 maps the locations of the Silk Road sites in the IAMC highlands.

Table 1: Count of Silk Road Sites by Country and Node Types

	AF	AF/CN	AM	CN	IN	KG	KG/CN	KZ	PK	TJ	TR	UZ	Total
Current Settlement	18	0	1	41	7	17	0	3	0	29	2	0	118
Former Settlement	0	0	0	7	0	1	0	0	0	1	0	0	9
Gorge	0	0	0	1	0	1	0	0	0	0	0	0	2
Halting Place	1	0	0	0	7	0	0	0	0	0	0	0	8
Land Waypoint	0	0	0	0	0	1	0	0	0	0	0	0	1
NA	21	0	0	33	8	15	0	4	6	11	1	6	105
Pass	1	1	0	1	0	2	1	1	1	1	0	0	9
Stream	0	0	0	0	0	1	0	0	0	1	0	0	2
Total	41	1	1	83	22	38	1	8	7	43	3	6	254

Notes: This table summarizes the final count of the Silk Road sites by country and node types. Data is from ICOMOS/OWTRAD and **?**.

Nighttime Lights: Measuring development at fine spatial scales and across countries using existing surveys is a challenging task. Thus, we use high-resolution satellite imagery instead to proxy economic development. First, we use nighttime lights data from two sources: 1) the Version 1 Nighttime VIIRS Day/Night Band (VIIRS-DNB) Composites for the year 2016 from the Earth Observation Group (EOG) at NOAA/NCEI, and 2) the Satellite 18 Year 2013 Version 4 DMSP-OLS Nighttime Lights Time Series.

The DMSP-OLS dataset provides the annual cloud-free composites of the night lights intensity, available in 30 arc-second geographic grid cells. We use the
"stable_lights.avg_vis" product, which filters out ephemeral events, such as fires. The data values range from 0 to 63. Meanwhile, the VIIRS-DNB dataset provides the annual composites of the night lights intensity, produced in 15 arc-second geographic grids. We use the "vcm-orm-ntl" product, which measures the cloud-free average radiance values, removing outliers to filter out the fire and ephemeral lights. The data contains the radiance values with units in nano Watts per square

Figure 2: Silk Road Sites in Inner Asia Mountain Corridor

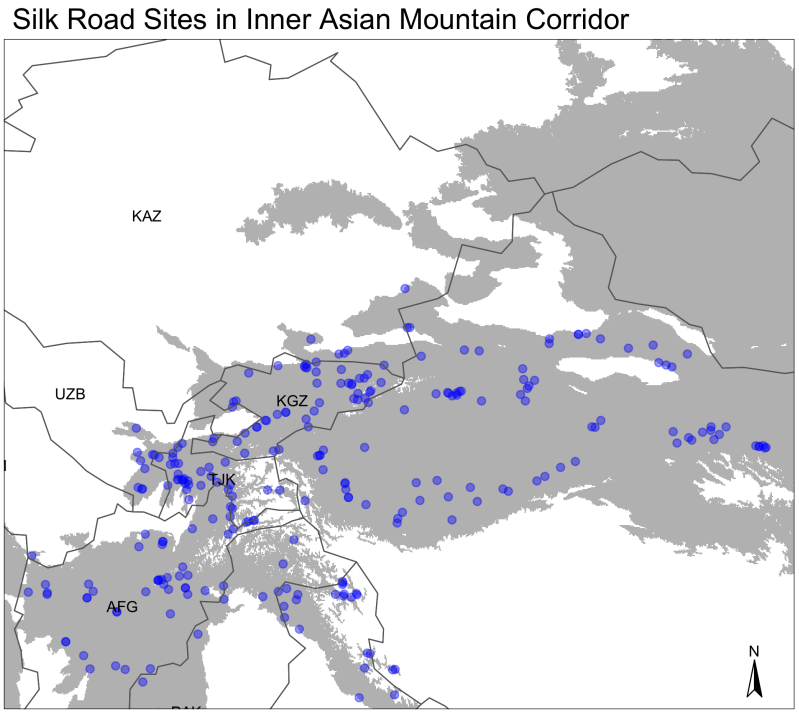

Notes: This figure presents Silk Road sites in the Inner Asia Mountain Corridor, as compiled by Old World Trade Routes (OWTRAD) Project (**?**) and **?**. The gray area represents the area of interest, i.e., the landmass of the IAMC that falls between 750m and 4,000m in elevation.

.

centimeter per steradian ($nanoWatts/cm^2/sr$). The VIIRS-DNB is considered to be superior to its predecessor DMSP-OLS, both in terms of spatial precision and low-light detection capabilities. We therefore consider the VIIRS-DNB dataset to be our preferred measurement.

The limitations with night lights data are well-known (**?**). Light spills over into adjacent grid cells, some lights are a result of gas flares instead of economic activity, and the light measurements are usually not sensitive enough to pick up on less dense activities, such as agriculture. Because of the limitation of night lights data, we supplement our measure of modern-day development with two additional measures of development, as detailed below.

Other Development Measures: We first supplement our measure of modern-day development with data on population density, which we obtain from the Gridded Population of the World (GPWv4) provided by the NASA Socioeconomic Data and Applications Center (SEDAC). GPWv4 uses data from the 2010 round of Population and Housing Census to model the distribution of the human population at a spatial resolution of 30 arc-seconds. We use the estimate of the population density for the year 2015, which provides the number of persons per square kilometer.

In addition to nighttime lights and population density data, we use land cover data from GlobeLand30-2020 as an alternative measure of modern development. GlobeLand30's classification system consists of ten land cover types, namely cultivated land, forest, grassland, shrubland, wetland, water bodies, tundra, artificial surfaces, bareland, and permanent snow and ice. Data is available at 30-m resolution.

Other Datasets: We supplement our data with other high-spatial-resolution data for our instrument and controls. We adopt the normalized difference vegetation index (NDVI) and the algorithm to simulate the seasonal mobility pattern of nomadic herders, both of which will be used for the construction of our instrumental variable, from (**?**). The NDVI data used is the 7-day average NDVI values in the month of August from eMODIS. We provide further details about the instrument in Section 4.3.

The data for the controls are standard in the literature. We use the caloric suitability index from **?**, which calculates the potential agricultural output based on crops that were available for cultivation in the time before 1500 CE. We also use the terrain ruggedness measure developed by **?** as well since terrain ruggedness could affect how suitable an area is for settlement. Lastly, we use AquaMaps for yearly precipitation and shapefiles of major rivers. We also add a selection of variables from the Global Agro-ecological Zones v3.0 (**?**), such as the crop suitability index and total production capacity in terms of tons per hectares for barley, flax, foxtail-millet, pearl-millet, rice and wheat.

Finally, we have a few other spatial datasets that we use to test for mechanisms. We use the Global Map of Irrigation Areas from FAO's AQUASTAT, which reports the percentage of irrigated land per cell size of 5 minutes worldwide as of 2005. Additionally, we use the 2015 Global Exposure

Database for GAR provided by the United Nations Office for the Coordination of Humanitarian Affairs. This dataset is primarily used to assess damage from disasters and includes estimates of various exposed capital stock worldwide at 1km spatial resolution. It includes the value of the capital stock, separated into categories such as housing, education, and health.

3.2 Data Construction

Since we are interested in the highland Silk Road along the Inner Asian Mountain Corridor, we limit the geographic extent of the study zone to 30 degrees to 55 degrees latitude and 60 degrees to 100 degrees longitude.[3] Additionally, we follow **?** in limiting the study zone between the elevations of 750 m and 4,000 m. Within the region of interest, we construct a regular 0.167×0.167 degrees grid, which corresponds to approximately 19×19 kilometers. We treat each grid cell as an observation. We construct the variables as follows.

Shortest Distance to Silk Road Site: We define a cell as a Silk Road cell if it contains at least one Silk Road site. We capture the distance from each grid cell to the Silk Road sites by measuring the distance[4] between the cell's centroid to the centroid of the nearest Silk Road cell. We call this the shortest distance from the cell to the Silk Road site.[5] Figure 3 plots the shortest distance measure that we construct.

Our choice to define the Silk Road based on the Silk Road sites rather than the Silk Road routes as established by historians is intentional. Despite the name "Silk Road," there were no physical roads that dictated specific routes of the Silk Road. Traditionally, historians established Silk Road routes by calculating the least-cost paths between pre-identified historical Silk Road sites. By construction, the Silk Road routes as established by historians are inherently dictated by ease of travel, which is endogenous to modern development. In this respect, defining the Silk Road based on the Silk Road routes is problematic for the purpose of this paper. Therefore, we define the Silk Road locations based on the Silk Road sites without imposing any routes between them.

Measure of Modern Level of Development: Nighttime lights data and population density data consist of continuous values. As such, we compute the variable value from those datasets by averaging the values across all pixels in a grid cell. The land cover dataset consists of categorical values and cannot be treated in the same manner. For each grid cell, we compute the percentage of the area that is classified as artificial surfaces, which are defined as "lands modified by human activities, including all kinds of habitation, industrial and mining area, transportation facilities, and interior urban green zones and water bodies, etc." A higher percentage of artificial surfaces signifies a higher level of urbanization and thus a higher level of development. Additionally, to account for the possibility that human activities in the region may consist primarily of agriculture,

[3] The range of interest for our study area is dictated by our instrument.
[4] We use the shortest distance along the earth's surface, also known as "as the crow flies" distance.
[5] We also construct an alternative measure as a robustness check. See Appendix B for details.

Figure 3: Shortest Distance to Silk Road site

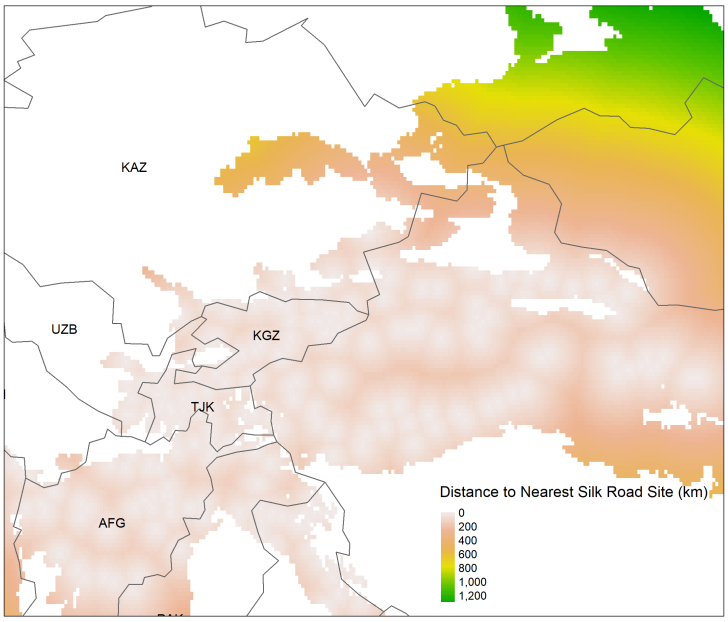

Notes: This figure displays the shortest distance between the centroid of each grid cell to the centroid of the nearest Silk Road cell.

we construct an alternative variable that measures the percentage of the area classified as cultivated land or artificial surfaces.

Table 2 presents the summary statistics of the development measures at the 0.167×0.167 degrees grid cells level. Given the presence of grid cells with zero value, we use the inverse-hyperbolic-sine (IHS) transformation before taking log in our subsequent analyses. This approach is consistent with what has been adopted in the literature (**??**).

Other Variables: All other non-distance variables are computed by averaging the values across all pixels in each grid cell. We construct all distance-related variables in the same manner as how we measure the shortest distance to the Silk Road. Variables containing zero are transformed using IHS transformation before taking log in the subsequent analyses.

4 Specification and Results

The relationship between ancient Silk Road trade and modern development can be represented by the following regression:

$$Y_i = \beta_0 + \beta_1 DistancetoSilkRoad_i + \beta_2' Z_i + \gamma_i + \varepsilon_i \quad (1)$$

Table 2: Summary Statistics of Development Measures

	Mean	Std. Dev.	Min	Max	Skewness	Kurtosis
VIIRS	0.04	0.57	0.00	40.10	46.95	2,703.67
DMPS	0.38	2.04	0.00	62.92	13.03	262.54
Population Density	27.76	134.70	0.00	7,423.69	25.13	980.31
Land cover (artificial surfaces)	0.00	0.02	0.00	0.92	19.58	565.77
Land cover (both)	0.06	0.15	0.00	1.00	3.71	17.56

Notes: This table reports the summary statistics of measures of development measures. One unit of observation is a 0.167 degrees by 0.167 degrees grid cell. Population density refers to the number of persons per square kilometer. Land cover (artificial surfaces) refers to the percentage of a grid cell that is covered by lands modified by human activities. Land cover (both) refers to the percentage of a grid cell that is classified as cultivated land or artificial surfaces.

where Y_i is a measure of modern development of grid cell i, $DistancetoSilkRoad_i$ is the shortest distance from grid cell i to the ancient Silk Road site, Z_i represents other control variables, and γ_i represents the country fixed effects. We control for the geographical features that can influence both the placement of Silk Road sites and modern development. Specifically, we control for the potential agricultural output, terrain ruggedness, distance to the nearest river, and elevation.

Analyzing the standard errors of the coefficients from our regressions is particularly important given that we are working with spatial data. Below, we first describe how we calculate the standard errors before presenting the results from our OLS regressions and introducing our instrumental variable approach.

4.1 Standard Errors

The First Law of Geography, written by **?**, states that "everything is related to everything else, but near things are more related than distant things." Spatial data is autocorrelated and thus must be taken into account in the empirical strategy. Unlike the literature that addresses standard errors and autocorrelation through time, the literature that addresses standard errors in the context of spatial autocorrelation has less consensus on what methods are best to minimize the influence of correlated noise on the results.

The common starting point is **?**'s paper, which outlines a process for generating spatial Heteroscedasticity and Autocorrelation Consistent (HAC) standard errors. **?**'s method is successful in curbing estimated t statistics, relative to robust standard errors, but is sensitive to the choice of kernel, bandwidth, and the unique spatial pattern of the data (**?**). Related research has shown that the choice of kernel is less important relative to the choice of bandwidth. This is because asymptotically, different kernel densities tend to converge to similar results (**?**). Thus, we focus on choosing a correct bandwidth, and then perform robustness checks on our regressions to confirm that the standard errors are of the correct magnitude.

There are three methods we consider to choose an optimal bandwidth. The first method is a simple rule-of-thumb proposed by (**?**). They suggest choosing a bandwidth b based on the following formula $b = n^{2\tau}$ where n is the number of observations, and $\tau \leq 1/3$. In our study, an observation is a grid cell, the size of which may be adjusted. Next, **?** suggest a data-driven cross-validation method performing the following minimization: $\min_b \sum_{i=1}^{n}(y_i - \hat{y}_{-i}(b))^2$ where $\hat{y}_i$ is the fitted value of y_i with location i omitted during the fitting process. **?** also suggest another data-driven approach of fitting a variogram to the data and setting the bandwidth as the generated range r, which is when the distance at which points are not significantly spatially correlated. Due to its straightforwardness and ease of interpretation, we use the last approach and fit a variogram (Figure 4), leading us to choose a bandwidth of 2 degrees.

Figure 4: Variogram

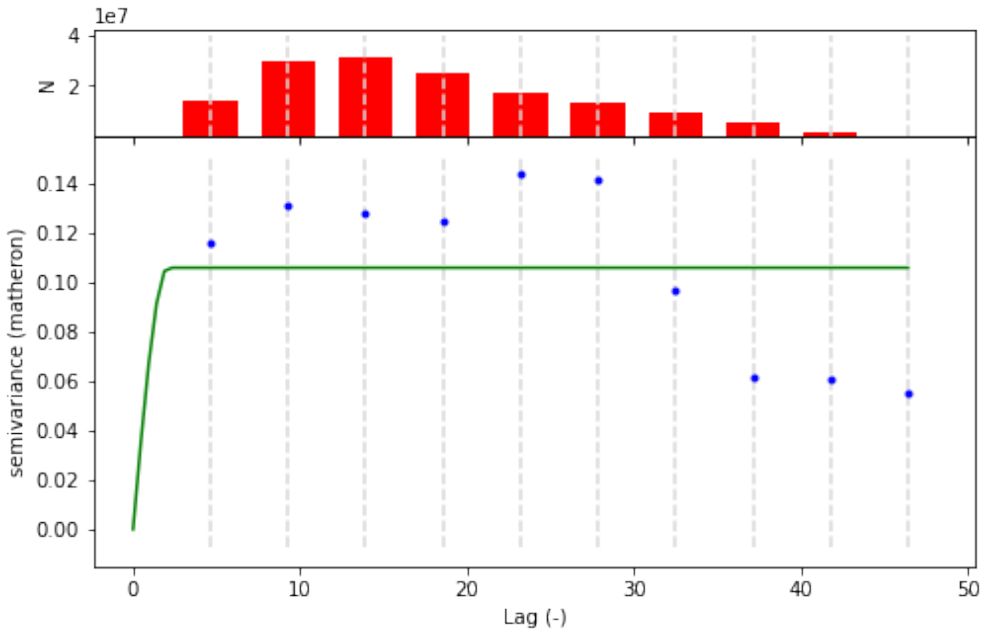

Notes: This figure presents the variogram that we generate to determine the bandwidth used to calculate spatial HAC standard errors. A variogram is a function that describes the degree of spatial dependence (y-axis) of a spatial field as the distance between two spatial units increases (x-axis). A variogram has three important parameters: the nugget n, the height of the variogram at the origin; the sill s (0), the spatial dependence value at which the curve begins to flatten (0.11); and the range r, the distance at which the curve begins to flatten (2.07). The range determines the bandwidth we will use when calculating the spatial HAC errors.

4.2 OLS Approach

Preliminary results from the OLS regressions are shown in Table 3 and Table 4. Table 3 shows the results when we use the VIIRS night lights as a proxy for modern level of development. Distance to Silk Road site is standardized and all other variables are log-transformed. The first column shows the relationship between night lights and distance to the nearest Silk Road site, controlling for only the country fixed effects and no additional control variables. There is a significant and negative relationship; as we increase the distance to the Silk Road site by one standard deviation, the night lights level falls by 2.3% on average.

Table 3: OLS Results

	(1)	(2)	(3)	(4)
	Night lights (VIIRS)			
Distance to Silk Road site	-0.023***	-0.036***	-0.034***	-0.032***
	(0.006)	(0.008)	(0.008)	(0.008)
Caloric suitability index		-0.001	-0.001	-0.001
		(0.001)	(0.002)	(0.002)
Ruggedness		-0.010***	-0.015***	-0.013***
		(0.004)	(0.003)	(0.003)
Precipitation		0.040***	0.011	0.016*
		(0.008)	(0.008)	(0.009)
Distance to river		-0.007***	-0.005**	-0.004**
		(0.002)	(0.002)	(0.002)
Elevation		-0.051***	-0.029**	-0.042***
		(0.012)	(0.011)	(0.014)
Crop-Suitability-Indices	No	No	Yes	Yes
NDVI	No	No	Yes	Yes
Latitude and longitude	No	No	No	Yes
Country FE	Yes	Yes	Yes	Yes
N	17,675	17,675	17,125	17,125

Notes: This table reports results from the OLS regression following equation (1). Distance to Silk Road site is standardized. All other variables are log-transformed. Standard errors are adjusted to allow for spatial clustering as in Conley (1999), with a bandwidth of 2 degrees using Bartlett kernel. Crop-suitability-indices include indices for wheat, rice, barley, flax, and millet. All regressions include a constant. *$p < 0.1$, ** $p < 0.05$, *** $p < 0.01$

The second column shows the relationship when we control for other factors that may affect modern level of development. We control the caloric suitability index, the ruggedness of the terrain, the amount of precipitation, the distance to the nearest river, and the elevation. In the third column, we control for land fertility more directly using the crop-suitability-index of major crops from the FAO GAEZ dataset. Specifically, we control for the crop-suitability-index of wheat, rice, barley, flax, and foxtail millet. Additionally, we control for the NDVI value of each grid cell. The controls used in this column constitute our baseline specification. **?** recommends accounting for the geographical location of the observations when studying the relationship between modern outcomes

and the historical characteristics of the places in the past. In the fourth column, we control for the latitude and the longitude of our observation in addition to the controls in our baseline specification. Generally, we can see that adding in controls does not significantly affect our coefficient of interest; the relationship between the night lights and the distance to the Silk Road sites is always negative and significant at 1%.

The majority of existing literature estimates the elasticity between night lights and GDP using the DMSP-OLS data. **?** estimate the elasticity using country-level data and find that the structural effect of true income growth on lights growth varies between 1.03-1.72, implying the elasticity of GDP with respect to night lights between 0.58-0.97. Similarly, **?** find the cross-country estimate to be 0.76.[6] Among the limited literature that studies the VIIRS-DNB data, **?** estimate the elasticity of GDP per capita with respect to night lights intensity using prefecture-level in China. They find that a 1% increase in night lights intensity corresponds to a 0.41-0.47% increase in GDP per capita.

Table 4 shows the results when we use alternative measures of modern development under our baseline specification. The negative relationship between distance to the Silk Road sites and modern level of development is significant across all measures. The first column shows that the coefficient of the distance to the Silk Road site is larger in magnitude when we use the DMSP night lights measure instead of the VIIRS night lights data. This is somewhat expected since the DMSP data has limited capability to detect lights at low radiance levels; therefore, the DMSP may have underestimated the level of night lights in areas with a lower level of economic activity, leading to an upward bias in the estimate. The second column shows the result when we use modern level of population to measure modern outcome. On average, a one standard deviation increase in distance to the Silk Road sites corresponds to a 49.8% decrease in population density.[7] The third and the fourth columns show the results when using data from the land cover data set as our dependent variable. In column 3, modern development is measured by the percentage of land that is covered by artificial surfaces, which are defined as areas that have artificial cover resulting from human activities such as construction. In column 4, the dependent variable is the percentage of land classified as artificial surfaces or cultivated land. On average, as the distance to the nearest Silk Road site increases by one standard deviation, the percentage of area covered by artificial surfaces decreases by 0.4%, and the percentage of area covered by artificial surfaces or cultivated land decreases by 6.2%.

4.3 Instrumental Variable Approach

Although regression (1) shows that proximity to Silk Road site corresponds to a higher level of modern development, one can still be concerned about other unobserved heterogeneity. To establish a causal relationship between the ancient Silk Road trade and modern development, we adopt an

[6]The paper finds that a one percentage point increase in GDP growth increases night lights growth by 1.317 percentage points, which implies an inverse elasticity of $1/1.317 = 0.76$.

[7]We find a stronger effect when we proxy for development using population density, which is in line with what has been found in the literature. For example, **?** found that a 10% increase in distance away from a portage predicts a 6% lower population density and 2% lower night lights intensity.

Table 4: OLS with Alternative Measures of Development

	(1)	(2)	(3)	(4)
	Night lights (DMPS)	Population density	Land cover (artificial surfaces)	Land cover (both)
Distance to Silk Road site	-0.157***	-0.689***	-0.004***	-0.064***
	(0.028)	(0.099)	(0.001)	(0.008)
Caloric suitability index	-0.013*	0.055**	-0.000	-0.007***
	(0.007)	(0.027)	(0.000)	(0.002)
Ruggedness	-0.068***	-0.048	-0.002***	-0.043***
	(0.011)	(0.047)	(0.000)	(0.005)
Precipitation	0.042	0.420***	0.001	0.019**
	(0.029)	(0.112)	(0.001)	(0.008)
Distance to river	-0.028***	-0.009	-0.000	-0.005***
	(0.006)	(0.018)	(0.000)	(0.002)
Elevation	-0.142***	-0.522***	-0.002	-0.017*
	(0.041)	(0.136)	(0.001)	(0.009)
Crop-Suitability-Index	Yes	Yes	Yes	Yes
NDVI	Yes	Yes	Yes	Yes
Latitude and longitude	No	No	No	No
Country FE	Yes	Yes	Yes	Yes
N	17,125	17,125	17,125	17,125

Notes: This table reports results from the OLS regression following equation (1) with alternative development measures as dependent variable. Distance to Silk Road site is standardized. All other variables are log-transformed. Standard errors are adjusted to allow for spatial clustering as in Conley (1999), with a bandwidth of 2 degrees using Bartlett kernel. Crop-suitability-indices include indices for wheat, rice, barley, flax, and millet. All regressions include a constant. *$p < 0.1$, ** $p < 0.05$, *** $p < 0.01$

instrumental variable strategy. A valid instrument is a variable that, after controlling for other controls in the regression, i) strongly correlates with the proximity to the Silk Road sites, and ii) only affects modern development level through the Silk Road.

4.3.1 Instrument: Seasonal Mobility Patterns of Nomadic Herders

To provide exogenous variation for the location of the Silk Road sites, we use two unique features of the Inner Asia Mountain Corridor and its inhabitants. First, ancient Silk Road traders wishing to travel between East Asia and the Mediterranean were obligated to use the overland routes in the IAMC. In the lowland regions, which were flatter and fertile with strong agricultural traditions, trading routes were generally selected based on ease of travel for traders. In the highland regions, because of the sparsely populated and often barren terrain in the highland area, the group of people who had generally traversed the area was the nomadic herders; subsequently, traders crossing the highland region followed the paths taken by the nomadic herders.

Second, unlike the traders, the nomadic herders' objective for moving overland was not to find the least-cost path of traversing the highland region to get to the lowland destination, but to exploit variation in the pasture quality as they traversed the highlands. The quality of pastures in the lowland and highland regions changes substantially over the seasons. In the summer months, lowland pastures become too arid while highland pastures become more productive. For over 4,500 years, nomadic herders have exploited these seasonal variations in pasture quality, moving from the lowland areas to the highland areas in the summer and returning to the lowland regions in the winter. **?** find that the seasonal mobility patterns of nomadic herders shaped the highland Silk Road networks. By following the footsteps of the nomadic herders, the traders were not taking the optimal path they should have taken if they simply wanted to cross the highland region to get to the lowland destinations.

Given that the highland Silk Road networks are shaped by the nomadic herders' seasonal mobility patterns and that the nomadic herders' movements are not dictated by the least-cost path of traversing the IAMC, the seasonal mobility patterns of the nomadic pastoralist provide variations in the locations of the highland Silk Road that are not dictated by the ease of travel. We therefore instrument for the locations of the Silk Road sites using the seasonal herding patterns. The exclusion restriction is that after controlling for the suitability of the area for growing agricultural crops, the seasonal herding patterns of the nomadic pastoralist only affect modern development through the Silk Road trade.

Actual historical herding patterns of nomadic pastoralists are unrecorded. We therefore proxy for the nomadic herders' herding paths using the simulated seasonal herding patterns from **?**. **?** uses flow accumulation modelling[8] to simulate the aggregated seasonal movements of herd animals across the IAMC using classified grass fodder quality as the input. The model simulates a figurative

[8]Named the 'pastoralist participation' model.

count of 'animals' flowing from one cell to another across the IAMC based on the pasture quality, which is categorized based on the NDVI values, over 20 human generations. The result is a flow accumulation measure that represents the simulated herding patterns. For more detail about its construction, please refer to Appendix A.1 or **?** directly. Figure 5 provides a visual representation of the distribution of simulated flow accumulation values across the IAMC. The resulting paths from these simulated flow accumulation values can be thought of the herding pattern of the nomads.

Figure 5: Simulated Herding Path

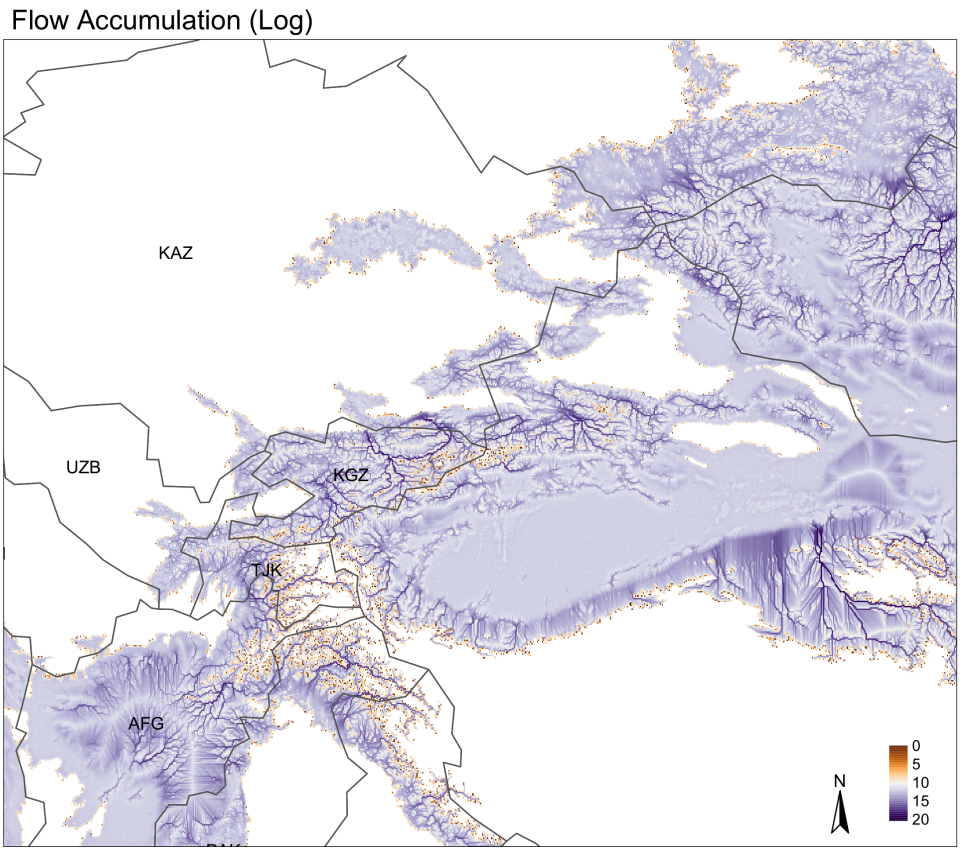

Notes: This figure presents the log flow accumulation values from the simulated season mobility pattern of nomadic herders in the Inner Asia Mountain Corridor as initially introduced and calculated by **?**.

The map of flow accumulation values is continuous. For computational feasibility, we must choose a cutoff for flow accumulation to isolate a pathway before constructing a distance to the flow accumulation path. We choose 1.5 million as a cutoff. Figure 6 shows the path generated. We later vary this cutoff to check the robustness of our results. After implementing this cutoff, the method to calculate the distance to the flow accumulation path is identical to the previous calculation of the distance to Silk Road site.

We argue that the simulated seasonal nomadic herding patterns satisfy the exclusion for the follow-

Figure 6: Simulated Herding Path and Silk Road Sites

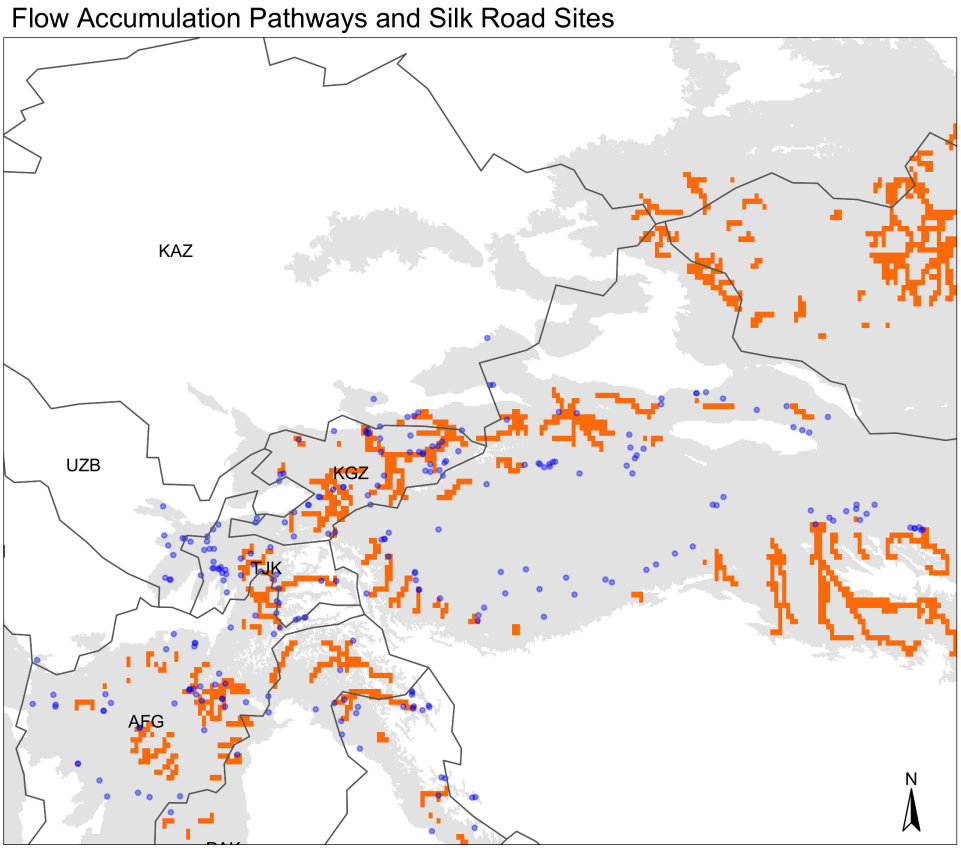

Notes: This figure presents the simulated herding paths generated using flow accumulation values of 1.5 million as a cutoff. The gray area represents the area of interest, i.e., landmass of the IAMC that falls between 750m and 4,000m in elevation.

ing reasons. First of all, nomadic mobility in the highland regions is primarily dicated by seasonal pasture quality rather than the 'ease of travel' (**?**). In fact, by construction, the simulated seasonal nomadic mobility is dictated by pasture quality and is not affected by typical factors that affect the ease of travel, such as slope. Secondly, the seasonal quality of pasture for grazing, which matters for the herders, does not translate to the productivity of land for farming, which is what matters for settlements. The highland region we are interested in is generally very rugged, making the entire area unsuitable for cultivation. As noted by Nunn and Puga (2012), cultivation becomes impossible when slopes are greater than 6; out of 36,000 cells in our region of interest, only 14 cells have a slope measure of less than 6. Therefore, the seasonal pasture quality that drives the nomadic herding patterns does not dictate the modern level of development of a certain location. Likewise, to further address concerns that pasture quality may correlate with the suitability of land for cultivation, we directly control for the suitability of land for various staple crops in our regressions using the FAO crop-suitability-indices. We also further directly control for the NDVI values in each grid cell. Thirdly, although nomadic herders move between lowland to highland areas over the year, they do not 'settle' permanently. Settlements, which matter for modern level of development, only took place as a result of trade through the Silk Road.

4.3.2 Instrumental Variable Results

Using the constructed distance to the flow pathways measure as an instrument, we run the following first-stage regression:

$$SilkRoad_i = \alpha_0 + \alpha_1 Flow_i + \alpha_2' Z_i + \lambda_i + \eta_i \tag{2}$$

where $Flow_i$ is the distance to the flow pathways measure that we constructed. We then use the predicted value $\widehat{SilkRoad}_i$ in the second-stage regression:

$$Y_i = \beta_0 + \beta_1 \widehat{SilkRoad}_i + \beta_2' Z_i + \gamma_i + \varepsilon_i \tag{3}$$

Table 5 shows the results from our IV specification. The first column shows the first stage result. The distance to the herding path positively correlates with the distance to the Silk Road sites, which is what we expect given **?**'s finding that the seasonal mobility patterns of nomadic herders shape the highland Silk Road networks. The F-statistic from our first stage is around 31.6, which is in the acceptable range for a strong instrument.

Columns (2)-(6) in Table 5 present the second stage results. The IV estimates are larger in magnitude than the OLS estimates, which can be explained by measurement errors in the locations of the Silk Road sites. From the IV regression, a one standard deviation increase in distance from the Silk Road site results in a 10.0% decrease in night lights intensity using the VIIRS-DNB data

Table 5: IV Results

	(1)	(2)	(3)	(4)	(5)	(6)
	First stage	Second stage				
	Distance to Silk Road site	Night lights (VIIRS)	Night lights (DMPS)	Population density	Land cover (artificial surfaces)	Land cover (both)
Distance to Silk Road site		-0.105***	-0.485***	-1.930***	-0.014***	-0.131***
		(0.029)	(0.107)	(0.365)	(0.004)	(0.025)
Distance to herding path	0.190***					
	(0.034)					
Caloric suitability index	-0.041***	-0.004**	-0.028***	-0.003	-0.001**	-0.010***
	(0.014)	(0.002)	(0.009)	(0.034)	(0.000)	(0.003)
Ruggedness	-0.048*	-0.018***	-0.083***	-0.103*	-0.003***	-0.046***
	(0.026)	(0.004)	(0.015)	(0.060)	(0.001)	(0.005)
Precipitation	0.255***	0.029**	0.125***	0.737***	0.003**	0.036***
	(0.047)	(0.011)	(0.040)	(0.138)	(0.001)	(0.010)
Distance to river	-0.026***	-0.005***	-0.031***	-0.020	-0.000*	-0.006***
	(0.007)	(0.002)	(0.007)	(0.020)	(0.000)	(0.002)
Elevation	0.021	-0.042***	-0.199***	-0.737***	-0.004*	-0.028**
	(0.106)	(0.016)	(0.060)	(0.213)	(0.002)	(0.012)
Crop-Suitability-Indices	Yes	Yes	Yes	Yes	Yes	Yes
NDVI	Yes	Yes	Yes	Yes	Yes	Yes
Country FE	Yes	Yes	Yes	Yes	Yes	Yes
F-stat	31.590					
N	17,125	17,125	17,125	17,125	17,125	17,125

Notes: This table reports results from the IV regressions. Distance to Silk Road site and distance to herding path are standardized. All other variables are log-transformed. Standard errors are adjusted to allow for spatial clustering as in Conley (1999), with a bandwidth of 2 degrees using Bartlett kernel. Crop-suitability-indices include indices for wheat, rice, barley, flax, and millet. All regressions include a constant. *$p < 0.1$, ** $p < 0.05$, *** $p < 0.01$

and 38.4% decrease in night lights intensity using the DMSP-OLS data.[9] Columns (4)-(6) present the IV results when we use alternative measures of modern development. The population density decreases by 85.5% with a one standard deviation increase in distance to the Silk Road site, while the percentage of area covered by artificial surfaces and the percentage of area covered by both artificial surfaces and cultivated land decrease by 1.4% and 12.3% respectively.

4.3.3 Robustness Checks

Random Sites: One could be concerned that the results in our analyses are driven by spatial noises. To ensure that this is not the case, we repeat our analyses using random sites instead of the Silk Road sites. Specifically, we generate the same number of random points in our region of interest as the number of Silk Road cells to represent random sites. We then calculate the shortest distance between the centroid of each grid cell to the centroids of the cells containing those random points, as illustrated in Figure 7.

We then reestimate the OLS equation (1) using the shortest distance to a random site instead of the shortest distance to a Silk Road site. The results are shown in the first column of Table 6. We do not observe a statistically significant relationship between the shortest distance to a randomly generated site and the intensity of night lights.

Least-cost mobility patterns of nomadic herders: Although our simulated herding patterns use pasture quality as the cost raster in the flow accumulation modeling, one could still be concerned that pasture quality may correlate with elevation, which would violate the exclusion restriction. To address this concern, we simulate the least-cost paths of the nomadic herders. Specifically, we generate new mobility patterns of the nomadic herders using the same flow accumulation modeling algorithm, but with the slope of the terrain as a cost raster in the model instead of pasture quality. Intuitively, this new generated path represents the hypothetical path we would expect 'animals' to take with a preference for a flatter slope. In the same manner as the construction of our instrument, we choose a cutoff of 1.5 million flow values for ease of computation. We then compute the shortest distance between each grid cell and the simulated least-cost paths of the herders.

Column 3 of Table 6 present the second-stage IV results after controlling for the shortest distance to the simulated least-cost paths of the herders. We can see that controlling for the least-cost paths of the herders does not significantly impact our IV estimate. Once we take into account the herders' least-cost paths, a one standard deviation increase in distance to Silk Road site corresponds to a 8.3% decrease in the night lights intensity, which is relatively similar to our baseline estimate of 10.0%.

[9] Our result is smaller than that in **?**, who found that night lights intensity is about 80% higher in cells within 50 km of the Silk Roads relative to cells that are 200-500 km away from the Silk Roads using DMSP-OLS data. This difference is somewhat expected since the area of study in **?** covers the lowland region of the Silk Road, where the routes are believed to be dictated by ease of travel and pass through big cities. Therefore, one would expect to see larger variations in night lights intensity in their paper.

Figure 7: Shortest Distance to Random Points

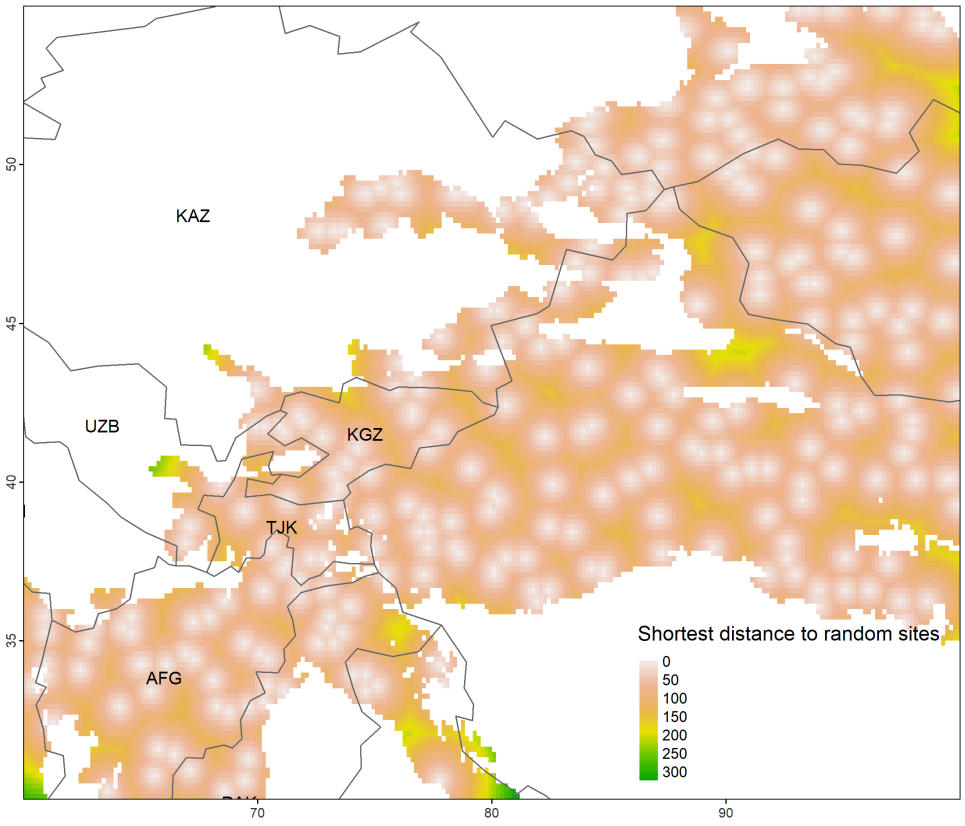

Notes: Shortest distance between the centroid of each grid cell and the centroid of the nearest cell with a randomly generated site. The number of randomly generated sites is the same as the number of the Silk Road cells present in the dataset.

Table 6: Robustness Checks

	(1)	(2)	(3)	(4)	(5)	(6)
	Night lights (VIIRS)	Distance to herding path	Night lights (VIIRS)	Distance to herding path	Night lights (VIIRS)	Night lights (VIIRS)
Distance to Silk Road site			-0.087**		-0.131***	
			(0.036)		(0.033)	
Distance to herding path		0.204***		0.199***		-0.001
		(0.054)		(0.034)		(0.001)
Distance to random site	-0.011					
	(0.013)					
Caloric suitability index	0.001	-0.041***	-0.003*	-0.023**	-0.003*	-0.000
	(0.002)	(0.014)	(0.002)	(0.011)	(0.002)	(0.000)
Ruggedness	-0.013***	-0.045*	-0.017***	-0.045**	-0.014***	-0.001
	(0.003)	(0.027)	(0.004)	(0.022)	(0.005)	(0.001)
Precipitation	0.002	0.266***	0.025**	0.294***	0.064***	-0.003
	(0.008)	(0.051)	(0.012)	(0.052)	(0.012)	(0.003)
Distance to river	-0.004**	-0.022***	-0.004**	-0.032***	-0.008***	-0.001*
	(0.002)	(0.007)	(0.002)	(0.008)	(0.002)	(0.001)
Elevation	-0.023**	-0.029	-0.047***	0.075	-0.060***	0.002
	(0.011)	(0.116)	(0.015)	(0.085)	(0.016)	(0.004)
Distance to herder's least-cost path		-0.000	-0.000			
		(0.000)	(0.000)			
Crop-Suitability-Indices	Yes	Yes	Yes	No	No	Yes
NDVI	Yes	Yes	Yes	No	No	Yes
Country FE	Yes	Yes	Yes	Yes	Yes	Yes
F-stat		14.278		34.271		
N	17,125	17,125	17,125	17,675	17,676	7,467

Notes: This table reports results from the robustness check exercises. Distance to Silk Road site, distance to herding path, and distance to random site are standardized. All other variables are log-transformed. Standard errors are adjusted to allow for spatial clustering as in Conley (1999), with a bandwidth of 2 degrees using Bartlett kernel. Crop-suitability-indices include indices for wheat, rice, barley, flax, and millet. All regressions include a constant. Column 1 shows the OLS results when we replace distance to Silk Road site with distance to randomly generated sites. Columns 2 and 3 show the IV results when we control for distance to herder's least-cost path. Columns 4 and 5 show the IV results when we exclude crop-suitability-indices and NDVI from the control variables. Column 6 shows the relationship between distance to herding path and night lights intensity when we only consider locations that are at least 150km away from the nearest Silk Road site. *$p < 0.1$, ** $p < 0.05$, *** $p < 0.01$

Excluding crop-suitability-indices and NDVI from control variables: Given that nomadic herders' mobility pattern is simulated using pasture quality as the input, one may be concerned that the variation in our instrument is all driven by agriculture-related factors. To verify that this is not the case, we exclude crop-suitability-indices and NDVI from our IV regressions. The fourth and fifth columns of Table 6 present the results. When we do not control for crop-suitability-indices and NDVI, a one standard deviation increase in distance to the nearest Silk Road site is associated with a 12.3% decrease in night lights, which is relatively close to our baseline estimate of 10.0%. The exclusion of crop-suitability-indices and NDVI does not significantly affect our results. Although the simulated herding path uses pasture quality as the input data, the actual simulation of the flow of animal stocks depends on the direction and the relative pasture quality. Nomadic herders move from locations with low pasture quality to locations with relatively higher pasture quality. The simulated herding path tracks their mobility pattern, crossing both places with low and high pasture quality. Our instrument is therefore not solely driven by agriculture-related factors.

Testing correlation between proximity herding path and development: We conduct an additional exercise to verify that proximity to herding path only affects modern development through the Silk Road. If herding path of the nomads only affects modern development through the Silk Road, we would expect to see no correlation between proximity to herding path and modern development in places where the Silk Roads are absent. We test this by only considering observations that are at least 150 km away from the nearest Silk Road site and run the OLS regression (1), replacing distance to Silk Road site with distance to herding path. The last column of Table 6 present the results. We can see that there is no significant relationship between proximity to herding path and night lights intensity in areas that are not in close proximity to the Silk Road. The result supports that proximity to herding path only affects modern development through the Silk Road.

Other robustness checks: We perform additional robustness checks, including using an alternative measure for proximity to Silk Road sites, excluding outliers, using different grid sizes, and using different cutoffs to construct our instrument. The results are reported and discussed in Appendix B.

5 Mechanisms

The results in the previous section indicate that the persistent impact of the ancient Silk Roads on modern development four centuries after the decline of the overland Silk Roads. However, what are the mechanisms through which the ancient trade routes impact the level of development in modern day? Night lights intensity itself is an indicator of economic activity. It does not answer why the ancient Silk Road's effects are persistent over time. In this section, we discuss two possible mechanisms: connectivity and capital investment.

Connectivity refers to the "connections" made between different places, which have endured over time. The ancient Silk Road both fostered new connections and strengthened existing connections across Eurasia. These connections may have persisted over time, even after the decline of the overland Silk Roads. Therefore, places that developed these connections as a result could remain more connected to markets today, and subsequently may be more developed and able to share new technologies more quickly. As time passes, this connectivity could manifest itself through stronger transportation network.

To explore the connectivity mechanism, we substitute distance to major roads in place of the nighttime lights intensity as a dependent variable. The first column of Table 7 presents the second stage results from the IV regression, using the shortest distance to a major road as a dependent variable. On average, as the distance to Silk Road increases by one standard deviation, the distance to a major road increases by 1.1 standard deviations. The result provides some evidence of the persistent effect of the Silk Roads arising from the connectivity mechanism.

Additionally, the persistent effect of the ancient Silk Roads may be a result of capital investment. Capital investment may refer to physical capital such as irrigation and urban development. As trade activity grew, investment in infrastructure in areas along the ancient Silk Road arose to service the traders. Even after the decline of the overland Silk Road trade, such infrastructure continued to be a source of agglomeration for subsequent economic activity and infrastructure investment. As a result, places along the ancient Silk Road could benefit from better irrigation and a higher density of health services.

To explore the investment mechanism, we substitute irrigation and building stock measures as a dependent variable in place of the nighttime intensity. Columns 2-6 of Table 7 report the results from the second stage IV regressions. The second column uses the (log) percentage of land equipped for irrigation as the dependent variable. Columns 3-6 use the (log) value of building stock used for housing, healthcare, education, and any purposes in that order. We consistently see a negative and significant relationship between distance to Silk Road site and measures of capital stock, indicating that capital investment and agglomeration could be one of the mechanisms through which the ancient Silk Roads affect modern development.

Our results in this section have shown a higher level of connectivity and capital investment in areas closer to the Silk Road. Note that both types of mechanisms may be acting in complementarity with each other, i.e., capital investment enhances connectivity, and connectivity enhances investment. Because of this, due to our current empirical strategy, we do not aim to disentangle one category of mechanism from each other, but provide suggestive evidence of their functioning.

Table 7: Mechanisms

	Distance to road	Irrigation	Building stock used for			
			Housing	Health	Education	All purposes
Distance to Silk Road site	1.087***	-1.252***	-1.656***	-0.192***	-1.236***	-2.141***
	(0.359)	(0.257)	(0.313)	(0.045)	(0.250)	(0.416)
Caloric suitability index	-0.008	-0.041	-0.072**	-0.012***	-0.039*	-0.084**
	(0.038)	(0.025)	(0.030)	(0.003)	(0.023)	(0.039)
Ruggedness	0.191***	-0.202***	-0.269***	-0.019***	-0.215***	-0.378***
	(0.053)	(0.038)	(0.047)	(0.006)	(0.037)	(0.062)
Precipitation	-0.594***	0.256***	0.484***	0.044***	0.361***	0.713***
	(0.168)	(0.093)	(0.115)	(0.014)	(0.090)	(0.156)
Distance to river	0.019	-0.105***	-0.146***	-0.011***	-0.112***	-0.197***
	(0.018)	(0.018)	(0.018)	(0.002)	(0.014)	(0.023)
Elevation	-0.217	-0.314**	-0.287*	-0.053**	-0.214*	-0.273
	(0.164)	(0.130)	(0.165)	(0.021)	(0.127)	(0.213)
Crop-Suitability-Indices	Yes	Yes	Yes	Yes	Yes	Yes
NDVI	Yes	Yes	Yes	Yes	Yes	Yes
Country FE	Yes	Yes	Yes	Yes	Yes	Yes
N	17,125	17,125	17,125	17,125	17,125	17,125

Notes: This table reports results from the second-stage IV regressions. Distance to Silk Road site and distance to road are standardized. All other variables are log-transformed. Standard errors are adjusted to allow for spatial clustering as in Conley (1999), with a bandwidth of 2 degrees using Bartlett kernel. Crop-suitability-indices include indices for wheat, rice, barley, flax, and millet. All regressions include a constant. *$p < 0.1$, ** $p < 0.05$, *** $p < 0.01$

6 Conclusion

The paper studies the long-term effect of trade routes on development. Using a novel instrument constructed from herding flows in the Inner Asia Mountain Corridor, this paper finds that locations along the highland Silk Road continue to be more developed centuries after the decline in the importance of ancient Silk Road overland trade corridors. The results are robust across different measures of modern development and different specifications.

Future work in this area may include studying further which types of Silk Road sites continue to have persistent effects on modern development over time and what mechanisms seem to be the most important. Another direction for work includes developing a theoretical model, including mechanisms, to explain the empirical link between the ancient Silk Road and modern development.

Simply, this study seeks to understand the effects of the past on the present and demonstrates that even choices made in antiquity, which dwindled in importance by the sixteenth century, still have enduring persistent effects on modern development today. Policymakers may consider that not only does the choice of a trade route or improvement in transportation have effects a decade later, but centuries later. Today, the ancient Silk Road is being revitalized in China's Belt and Road Initiative, which was introduced in 2013. Along with concentrating on maritime shipping lanes ("roads"), the Chinese government has identified several overland corridors ("belts") that they will target for development. One of these overland corridors is called the China-Central Asia–West Asia Economic Corridor (CCWAEC), a geographic area that encompasses the Inner Asia Mountain Corridor. Our study could have important implications for such an initiative.

References

Appendices

A Data

A.1 Constructing Flow Accumulation

The flow accumulation measure is the key simulated quantity that forms the basis of our instrumental variable strategy. It was introduced by **?** and, in simple terms, is a sum of seasonal nomadic migrations over 20 human generations. We briefly describe its construction.

? first construct their three base raster datasets. First, using Global Multi-Resolution Terrain Elevation Data (GMTED2010) with a pixel resolution of 30 arcseconds (about 1 km) within the inner Asian corridor, the researchers define the lowland and highland boundary at 750 m elevation. Next, they use a multispectral eMODIS image transformed into Normalized Difference Vegetation Index (NDVI) values from August 2008 at the peak of the grassland productivity to generate an NDVI raster averaged over seven days. Using this averaged NDVI raster and further information on fodder value and range productivity of biologically documented highland pasture types, the authors assign vegetation classes to each cell. Last, using the two most fertile classes of vegetation, they also create an animal weight raster which corresponds to 16 animals per hectare, the average range capacity for inner Asian highland grasslands.

Botanical and archaeological evidence suggests that despite climate and geographical change over Central Asia in the past 4000 years, the grassland vegetation is mostly unchanged (**?**). Thus, modern imagery like eMODIS to calculate NDVI and modern measures of highland pasture productivities may be used to simulate historical flow accumulation measures.

Having constructed their base rasters, **?** begin their recursive algorithm. The following steps are iterated 500 times to simulate 500 years of flow patterns. First, they randomly generate 5,000 lowland campsites. Using these campsites as sources and the vegetation classes generated previously as weights, the researchers apply the "Cost Distance" tool in ArcGIS to generate a cost distance raster. The cost distance raster gives the distance, for each grid cell, to the nearest campsite for each cell in the raster based on the least-accumulative cost. The cost distance raster, which was calculated using measures of pasture quality, and the animal weight raster are then used as inputs to the ArcGIS tool "Flow Accumulation", which produces a hypothetical count of animals flowing from the best pastures into each cell across the highlands region. Reverse flows are prohibited. This final raster is the flow accumulation measure (Figure 5) that we use in this paper.

B Robustness Checks

In this section, we present the additional robustness checks that we perform. All our robustness checks reported below use our baseline IV specification with the VIIRS night lights data as a measure of modern development.

Excluding outliers: We first exclude outliers from our analysis. To ensure that the negative relationship between proximity to Silk Road site and modern development is not driven by the extreme values in the data, we exclude observations with VIIRS values in the top and bottom 2 percentiles from our analysis. The first two columns of Table B.1 present results. We still observe a negative and significant relationship between proximity to Silk Road site and night lights intensity after excluding the outliers.

Alternative measure of proximity to the Silk Road: In our analyses throughout the paper, we use the shortest distance to the nearest Silk Road site as a measure of proximity to the Silk Road. As a robustness check, we construct an alternative measure by constructing the variable c_{di}, which measures the number of Silk Road cells that can be reached within distance d from cell i. We call this the connectedness of cell i to the Silk Road.[10] We show this measure in Figure B.1, in which we use 100km as a distance cutoff.

Figure B.1: No. of Silk Road cells within 100km

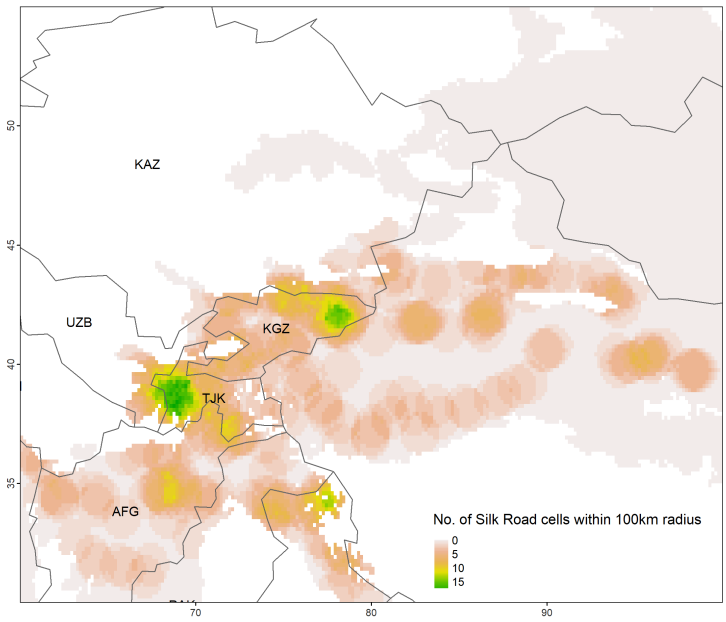

Notes: This figure presents the number of Silk Road cells within 100km radius.

We then use this connectivity measure in place of our standard distance to Silk Road site measure.

[10] This measure is similar to the one used in **?**.

Table B.1: Robustness Checks

	(1)	(2)	(3)	(4)	(5)	(6)	(7)	(8)
	Excluding outlier		Using connectivity measure		Using 0.083×0.083 degree cells		Using 4.167×4.167 degree cells	
	Distance to Silk Road site	Night lights (VIIRS)	Distance to Silk Road site	Night lights (VIIRS)	Distance to Silk Road site	Night lights (VIIRS)	Distance to Silk Road site	Night lights (VIIRS)
Distance to Silk Road site		-0.028***				-0.088***		-0.117***
		(0.007)				(0.025)		(0.028)
No. of Silk Road cells within 100 km				0.106***				
				(0.026)				
Distance to herding path	0.182***		-0.189***		0.181***		0.230***	
	(0.036)		(0.041)		(0.034)		(0.030)	
Caloric suitability index	-0.046***	-0.002***	0.051**	-0.005*	-0.033**	-0.004**	-0.061***	-0.006**
	(0.016)	(0.001)	(0.023)	(0.003)	(0.013)	(0.002)	(0.018)	(0.003)
Ruggedness	-0.053*	-0.005***	0.043	-0.018***	-0.038	-0.015***	-0.081***	-0.018***
	(0.028)	(0.001)	(0.027)	(0.004)	(0.024)	(0.003)	(0.030)	(0.006)
Precipitation	0.259***	0.007***	-0.042	0.006	0.249***	0.024***	0.292***	0.032**
	(0.050)	(0.003)	(0.071)	(0.009)	(0.048)	(0.009)	(0.051)	(0.015)
Distance to river	-0.025***	-0.002***	0.015	-0.004**	-0.027***	-0.005***	-0.028***	-0.008**
	(0.007)	(0.001)	(0.011)	(0.002)	(0.007)	(0.001)	(0.008)	(0.003)
Elevation	0.016	-0.012***	-0.181*	-0.025*	0.006	-0.035***	0.059	-0.035*
	(0.116)	(0.004)	(0.107)	(0.013)	(0.107)	(0.013)	(0.109)	(0.019)
Crop-Suitability-Indices	Yes	Yes	Yes	Yes	Yes	Yes	Yes	Yes
NDVI	Yes	Yes	Yes	Yes	Yes	Yes	Yes	Yes
F-stat	25.785		21.488		27.870		60.212	
N	15,732	15,733	17,125	17,126	65,305	65,306	2,984	2,984

Notes: This table presents results from additional robustness check exercises. Distance to Silk Road site, distance to herding path, and number of Silk Road cells within 100km are standardized. All other variables are log-transformed. Standard errors are adjusted to allow for spatial clustering as in Conley (1999), with a bandwidth of 2 degrees using Bartlett kernel. Crop-suitability-indices include indices for wheat, rice, barley, flax, and millet. All regressions include a constant. $^*p < 0.1$, $^{**}p < 0.05$, $^{***}p < 0.01$

The results are reported in the third and fourth columns of Table B.1. As expected, there is a positive relationship between the connectedness to the Silk Road and the intensity of the night lights. As the number of Silk Road cells within 100km increases by one standard deviation, the night lights intensity increases by 11.2%.

Alternative grid sizes: Our baseline unit of observation is a 0.167 degrees $\times$0.167 degrees grid cell. We now check if our results are robust to the sizes of the cells. We first construct an alternative dataset using 0.083 degrees $\times$ 0.083 degrees grid cells, which is half the width and height of our baseline grid cells. Columns 5 and 6 of Table B.1 report the results. We then consider an alternative dataset with grid cells that are 25 times the width and height of our baseline grid cells. The results are shown in columns 7 and 8 of Table B.1. Overall, our results are robust to different cell sizes.

Constructing instrument with different cutoffs: Due to computational feasibility, we set a flow value of 1.5 million as a cutoff to construct the instrument in this paper. We now check the robustness of our results to different cutoff values. Table B.2 shows the results when we construct the instrument using 1 million and 2 million as our cutoff values. Our result is robust to different cutoff values.

Table B.2: IV Results Using Different Cutoffs to Construct an Instrument

	1 million cutoff		2million cutoff	
	First stage Distance to Silk Road site	Second stage Night lights (VIIRS)	First stage Distance to Silk Road site	Second stage Night lights (VIIRS)
Distance to Silk Road site		-0.093***		-0.111***
		(0.025)		(0.033)
Distance to herding path	0.204***		0.171***	
	(0.029)		(0.036)	
Caloric suitability index	-0.042***	-0.004*	-0.042***	-0.005**
	(0.014)	(0.002)	(0.014)	(0.002)
Ruggedness	-0.047*	-0.017***	-0.049*	-0.018***
	(0.026)	(0.004)	(0.026)	(0.004)
Precipitation	0.258***	0.026**	0.256***	0.030**
	(0.047)	(0.011)	(0.048)	(0.012)
Distance to river	-0.025***	-0.005***	-0.025***	-0.005***
	(0.007)	(0.002)	(0.007)	(0.002)
Elevation	0.045	-0.039***	0.002	-0.043***
	(0.103)	(0.015)	(0.106)	(0.016)
Crop-Suitability-Indices	Yes	Yes	Yes	Yes
NDVI	Yes	Yes	Yes	Yes
Country FE	Yes	Yes	Yes	Yes
F-stat	49.635		23.072	
N	17,125	17,125	17,125	17,125

Notes: This table presents results from additional robustness check exercises. Distance to Silk Road site and distance to herding path are standardized. All other variables are log-transformed. Standard errors are adjusted to allow for spatial clustering as in Conley (1999), with a bandwidth of 2 degrees using Bartlett kernel. Crop-suitability-indices include indices for wheat, rice, barley, flax, and millet. All regressions include a constant. *$p < 0.1$, ** $p < 0.05$, *** $p < 0.01$